Generalized Frenkel-Kontorova model: A diatomic chain in a sinusoidal potential

Aiguo Xu
CCAST (World Laboratory), P.O. Box 8730, Beijing 100080, People's Republic of China;
Graduate School, China Academy of Engineering Physics, P.O. Box 8009-30, Beijing, 100088, People's Republic of China;
and International Center for Materials Physics, Academia Sinica, Shenyang, 110015, People's Republic of China

Guangrui Wang and Shigang Chen
Center for Nonlinear Studies, Institute of Applied Physics and Computational Mathematics, P.O. Box 8009-28, Beijing 100088, People's Republic of China

Bambi Hu
Department of Physics and Center for Nonlinear and Complex System, Hong Kong Baptist University, Kowloon Tong, Hong Kong
and Department of Physics, University of Houston, Houston, Texas 77204
(Received 24 December 1997)

To understand modulated structures and commensurate-incommensurate transitions, we generalize the Frenkel-Kontorova model to a diatomic chain in the presence of an external sinusoidal potential. For the classical ground states, the diatomic effects are reflected by the phase diagram and the phonon spectrum. For the quantum ground states, the diatomic effects are reflected by the distribution of atoms on the external potential, the phase diagram, correspondences between the ground states and the orbits of the area-preserving maps, the phonon spectrum, and the occurrence of a second critical point K_c' besides K_c at which a transition by breaking analyticity occurs. [S0163-1829(98)06325-5]

I. INTRODUCTION

Various nonlinear phenomena in condensed matter physics can be described by a model where a chain of interacting particles is placed in a channel.[1] Such a model arises when one can pick out a one-dimensional subsystem from the whole system and consider the rest of the system as the source of an external potential, and, at the same time, as a thermal bath supporting an energy exchange with the subsystem of interest. If one ignores displacements of the particles in transverse directions and allows the particles to move only along the direction of the chain, the model reduces to a variant of the famous Frenkel-Kontorova[2] (FK) model. The FK model describes a chain of atoms connected by harmonic springs in the presence of a sinusoidal external potential. The FK model has been used to describe superionic conductors,[3] crowdions,[4] submonolayer films of atoms adsorbed on furrowed or stepped crystal surfaces,[5] and hydrogenbonded systems along channels in biomembranes.[6] Furthermore, the FK model is used to describe nonlinear phenomena such as dislocation dynamics, charge-density waves, ferroelectric domain walls, magnetically ordered structures, and commensurate-incommensurate (CI) transitions. To understand the modulated phases and laws of CI transitions, the standard FK model has been generalized to ones with nonharmonic interactions and/or nonsinusoidal external potential. The FK-type models have been extensively studied by S. Aubry,[7] S. N. Coppersmith and D. S. Fisher,[8] O. Biham and D. Mokamel,[9] and B. Hu, *et al.*,[10] when the interparticles' interactions are convex. R. B. Griffiths and W. Chou[11] present the effective potential method that can be applied to the study of the FK-type models with nonconvex interparticles' interactions. Such models are studied by A. Banerjea and P. L. Taylor,[12] M. Marchand and co-workers,[13] C. O. S. Yokoi and co-workers,[14] and A. Xu, *et al.*[15] The models with a transverse degree of freedom are studied by O. Braun and co-workers.[16] Several attempts to study the quantum effects of the FK model are also made.[17–19] These studies are restricted to simple lattice systems. S. Aubry and co-workers[20] studied a variation of the discrete FK model with two sublattices. In their model the atoms of the first sublattice that have even indices $2i$ are submitted to a periodic potential $V(x)$ with period $2a$; the atoms of the second sublattice that have odd indices $(2i+1)$ are submitted to the same period potential $V(x+a)$ shifted by half a period a, where $V(x)$ is piecewise parabolic. In addition the atoms are submitted to a staggered field with amplitude E. F. Axel and S. Aubry[21] studied a model representing a one-dimensional elastic chain of atoms subjected to a staggered electric field and a cosine potential. Some classical properties are given. Within all the studies mentioned above, all the atoms in the chain are identical.

Up to now, we know very little about the FK-type models with different atoms. The diatomic chain is very important in solid physics. It relates to the acoustic wave and the optical wave and is a typical model studying the lattice vibration. In this paper, we generalize the standard FK model to a diatomic chain in the presence of a sinusoidal external potential, and study its ground states in the classical and quantum frameworks, respectively. Two subjects will be discussed in the present paper. One is the phase diagram in the (γ,K) parameter space, in which the winding number of the ground state varies from one tongue to another. The other is the transition for a particular state with the golden mean winding number when K is varied. Most of the results occur in the quantum framework.

We present the results of our studies in four sections. The model is given and its classical properties are discussed in Sec. II. We study the quantum properties of the model in Sec. III. Section IV is the conclusion of the present paper.

II. CLASSICAL PROPERTIES OF THE MODEL

The generalized FK model used in this paper is described by the following Hamiltonian:

$$H=\sum\left(\frac{p_i^2}{2\mu_i}+\frac{1}{2}(x_i-x_{i-1}-\gamma)^2-\frac{K}{(2\pi)^2}\cos(2\pi x_i)\right), \tag{2.1}$$

where x_i and p_i are the coordinate and the momentum of the ith atom, γ is the nature length of the harmonic spring, and μ_i is the effective mass of the ith atom. The chain is composed of two kinds of atoms that are denoted by A and B, respectively. Without losing the generality, we let $\mu_i=\mu_A=1$ if i is an odd number and let $\mu_i=\mu_B=\mu$ if i is an even number. As in our previous studies,[15] we define the winding number of the whole system ω as

$$\omega=P/Q, \tag{2.2}$$

where Q is the period of the ground state and P is the period number of the external potential between the 1st and the $(Q+1)$th atoms. Similarly, we define the winding number of the Γ subsystem ω_Γ as

$$\omega_\Gamma=P_\Gamma/Q_\Gamma, \tag{2.3}$$

where Q_Γ is the period of the Γ subsystem, P_Γ is the period number of the external potential between the 1st and the $(Q_\Gamma+1)$th Γ atoms. Here $\Gamma=A$ or $\Gamma=B$. For the subsystems of the prensent model, there is no common divisor between P_Γ and Q_Γ, so this definition is equivalent to the traditional definition of the winding number.

A. Phase diagram and transition by breaking of analyticity

The two subchains have the same winding number, i.e., $\omega_A=\omega_B$, and the winding number of the whole chain is one half of that of the subchains, i.e., $\omega=\frac{1}{2}\omega_A=\frac{1}{2}\omega_B$. At zero temperature, $p_i=0$ for all the atoms, so the Hamiltonian of the system is just identical to that of the standard FK model that has been extensively studied. If we describe the ground state using the winding number of the whole chain, then the classical phase diagram of the present model can be readily obtained from that of the standard FK model in the following way: The phase diagram is just the same as that of the standard FK model in appearance. In a tongue with $\omega=P/Q$ for the standard FK model, if Q is an even number, then $\omega=P/Q$ and $\omega_A=\omega_B=P/(Q/2)$ for the present model; if Q is an odd number, then $\omega=2P/2Q$ and $\omega_A=\omega_B=2P/Q$ for the present model. From above analysis, we can find that the values of the winding numbers for the whole chain conform to the Farey tree structure, so $0\leqslant\omega\leqslant1$; the values of the winding numbers for the subchains do not conform to the Farey tree structure and they may be greater than 1.

For the classical incommensurate ground state of the present model, the position of the ith atom can be described by a hull function,

$$x_i=f(i\omega+\alpha), \tag{2.4}$$

which is just the same as that of the standard FK model. A *transition by breaking of analyticity* occurs at the same critical point K_c as the standard FK model. At $K=K_c$, the hull function describing the incommensurate structure undergoes a transition from an analytic function to a nonanlytic function. Many physical quantities also undergo a transition at K_c. In the following sections, we study three quantities: the phonon gap, the coherence length, and the Peierls-Nabarro barrier, for the ground state with the golden mean winding number.

B. Phonon gap, coherence length, and Peierls-Nabarro barrier

The gap in the phonon spectrum Ω_G is defined as the lowest phonon frequency in the system. For the system described by Eq. (2.1), consider a small vibration of the atoms around their equilibrium positions $\{x_i\}$,

$$x_i(t)=x_i+\epsilon_i(t). \tag{2.5}$$

The equation of motion for this vibration is described by

$$\mu_i\frac{d^2x_i(t)}{dt^2}=-\frac{\partial H\{[x_i(t)]\}}{\partial x_i(t)}. \tag{2.6}$$

The linearized equation of the motion for small vibration is given by

$$\delta\ddot{x}_i(t)+\sum_j\frac{1}{\mu_i}\frac{\partial^2H\{[x_i(t)]\}}{\partial x_i(t)\partial x_j(t)}\delta x_j(t)=0,\quad i=1,2,\cdots,Q, \tag{2.7}$$

where $\ddot{x}=d^2x/dt^2$ and

$$\frac{\partial^2H}{\partial x_i\partial x_j}=\begin{cases}-1, & j=i-1,\\ 2+K\cos(2\pi x_i), & j=i,\\ -1, & j=i+1.\end{cases} \tag{2.8}$$

The time Fourier transform of Eq. (2.7) gives

$$-\frac{\epsilon_{i-1}}{\mu_i}+\left(\frac{2+K\cos(2\pi x_i)}{\mu_i}-\Omega^2\right)\epsilon_i-\frac{\epsilon_{i+1}}{\mu_i}=0,$$
$$i=1,2,\cdots,Q. \tag{2.9}$$

Define a function, $D(x)=2+K\cos(2\pi x)$, then the eigenvalue equation (2.9) can be written as

$$\begin{bmatrix}\frac{D(x_1)}{\mu_1}-\Omega^2 & -\frac{1}{\mu_1} & 0 & \cdots & -\frac{1}{\mu_1}\\ -\frac{1}{\mu_2} & \frac{D(x_2)}{\mu_2}-\Omega^2 & -\frac{1}{\mu_2} & \cdots & 0\\ & & \vdots & & \\ -\frac{1}{\mu_q} & 0 & 0 & \cdots & \frac{D(x_q)}{\mu_q}-\Omega^2\end{bmatrix}=0, \tag{2.10}$$

with the periodic boundary conditions $x_0 = x_Q - P$ and $x_{Q+1} = x_1 + P$.

The hull function $x_i = f(i\omega + \alpha)$ is a static solution of equation $\partial H/\partial x_i = 0$ for any phase α. For $K < K_c$, since $f(x)$ is an analytic function, inserting this solution in $\partial H/\partial x_i = 0$ and differentiating this equation with respect to the phase α shows that

$$\epsilon_i = f'(i\omega + \alpha) \tag{2.11}$$

is a solution of Eq. (2.9) for $\Omega^2 = 0$. Consequently, for $K < K_c$ the gap in the phonon spectrum vanishes. The corresponding zero-frequency mode is the phason mode of the incommensurate structure for the generalized FK model.

In contrast, for $K > K_c$, the hull function $f(x)$ becomes discrete with a derivative which is zero almost everywhere. Therefore Eq. (2.11) no longer defines an eigenmode for Eq. (2.9) with $\Omega^2 = 0$ and the gap in phonon spectrum Ω_G does not necessarily vanish. Similar to standard FK model, we expect Ω_G behaves as

$$\Omega_G(K) \sim (K - K_c)^{\chi}. \tag{2.12}$$

Figure 1 shows some examples of the phonon spectrums, where $\omega = \frac{89}{144}$ for the whole chain, phonon spectrums 1, 2, and 3 are for the case of $\mu = 1$, $\mu = 0.5$ and $\mu = 3$, respectively. $K = 0$ in (a), $K = 0.8$ in (b), and $K = 1.5$ in (c). It is clear that phonon frequencies decrease with the increasing of μ. When $0 \leqslant K < K_c$, all the spectrums start from the origin point. When $K = 0$, spectrum 1 is roughly smooth while spectrums 2 and 3 are divided into two segments, respectively. Segments OA and OD correspond to the acoustic wave, BC and EF correspond to the optical wave, which is a well-known property of the diatomic chain. When $K > 0$, all the spectrums are divided into many segments. When $K > K_c$, all the minimum phonon frequencies are greater than zero. For the incommensurate state with the golden mean winding number $[\omega = (\sqrt{5} - 1)/2]$, the numerical results show that χ is just the same as that of the standard FK model, i.e., $\chi = 0.99 \pm 0.01$, though the phonon spectrums are different for different μ.

The coherence length ξ measures the distance over which a perturbation δx_n propagates along the chain. For instance, an infinitesimal displacement ϵ_0 at x_0 will cause a displacement ϵ_i at x_i,

$$\epsilon_i \sim \exp(-|i|/\xi)\epsilon_0, \tag{2.13}$$

where ξ is called the coherence length. When $K < K_c$, $\xi = \infty$. When $K > K_c$, $\xi = 1/\gamma$, where γ is the maximum Lyapunov exponent. The Peierls-Nabarro (PN) barrier of the grond state is defined as to be the minimal energy barrier that must be overcome to continuously translate the chain of atoms on the external potential. For the incommensurate state with $\omega = (\sqrt{5} - 1)/2$, the behaviors of the coherent length and PN barrier are just the same as those of the standard FK model.

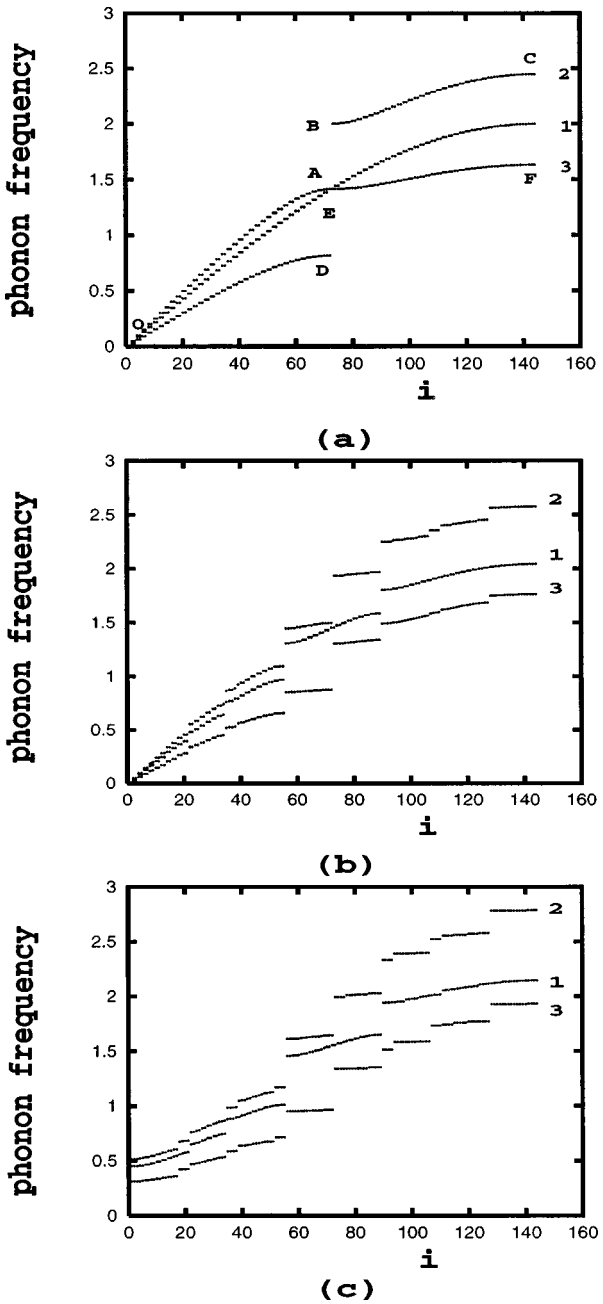

FIG. 1. Examples of the phonon spectrums, where $\omega = \frac{89}{144}$, phonon spectrums 1, 2, and 3 are for the case of $\mu = 1$, $\mu = 0.5$, and $\mu = 3$, respectively. $K = 0$ in (a), $K = 0.8$ in (b), and $K = 1.5$ in (c). It is clear that phonon frequencies decrease with the increasing of μ. When $0 \leqslant K < K_c$, all the spectrums start from the origin point. When $K = 0$, spectrum 1 is roughly smooth while spectrums 2 and 3 are divided into two segments, respectively. Segments OA and OD correspond to the acoustic wave, BC and EF correspond to the optical wave, which is a well-known property of the diatomic chain. When $K > 0$, all the spectrums are divided into many segments. When $K > K_c$, all the minimum phonon frequencies are greater than zero.

III. QUANTUM PROPERTIES OF THE MODEL

In the quantum mechanism, the mechanical quantities are described by Hermitian operators. The Hamiltonian operator of the system is

$$\hat{H} = \sum \left(\frac{\hat{P}_i^2}{2\mu_i} + \frac{1}{2}(\hat{X}_i - \hat{X}_{i-1} - \gamma)^2 - \frac{K}{(2\pi)^2}\cos(2\pi\hat{X}_i) \right). \tag{3.1}$$

Because of the existence of the interatomic interactions and the external potentials, the classical ground state is uniquely

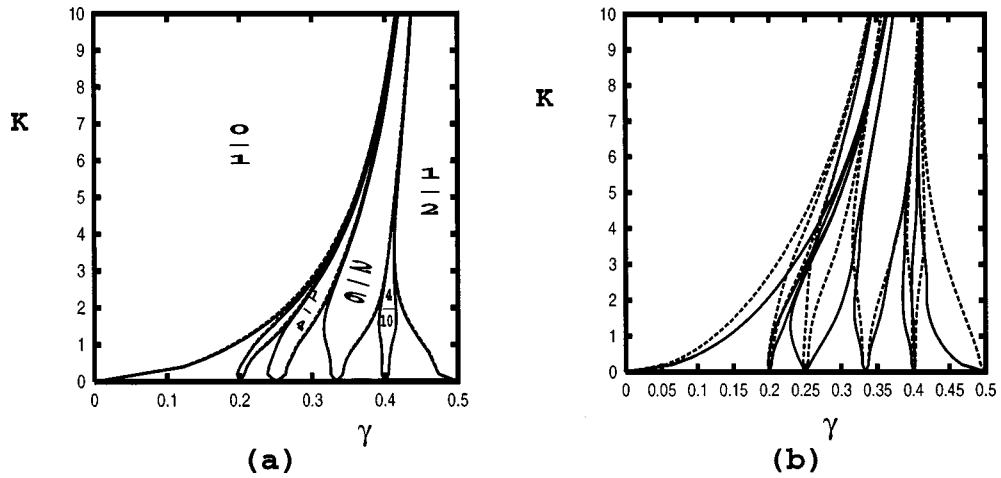

FIG. 2. Examples of the phase diagrams, where only the tongues with $Q_A=Q_B\leqslant 5$ are shown. The tongues limited by the dashed lines are for the case of $\mu=1$, the tongues limited by the solid lines are for the case of $\mu=5$. From left to right, the winding numbers for the whole chain are $\frac{0}{1}$, $\frac{2}{10}$, $\frac{1}{4}$, $\frac{2}{6}$, $\frac{4}{10}$, and $\frac{1}{2}$, respectively. $\hbar=0.01$ in (a) and $\hbar=0.1$ in (b). It is clear that when $\hbar$ is very small the boundaries of the corresponding tongues nearly coincide.

determined. In the quantum mechanism, the ground state is in a bound state. Owing to the quantum fluctuation, one of the physical quantities of interest is the expectation value of the corresponding operator. The coordinate and momentum operators for the ith atom are written as

$$\hat{X}_i=\sqrt{\frac{\hbar}{2\sqrt{\mu_i}}}(a_i^+ + a_i),$$
$$\hat{P}_i=i\sqrt{\frac{\hbar\sqrt{\mu_i}}{2}}(a_i^+ - a_i), \tag{3.2}$$

where a_i^+ and a_i are boson creation and annihilation operators that satisfy the canonical commutation relations: $[a_i,a_j^+]=\delta_{ij}$, $[a_i,a_j]=0$, $[a_i^+,a_j^+]=0$. We use the variational method[19] to study the ground state of system (3.1) in the framework of the coherent state theory. We use the coherent state, $|\Psi\rangle=D(\alpha)|0\rangle$, as the trial wave function of the ground state, where $D(\alpha)=\exp(\alpha_i a_i^+ - \alpha_i^* a_i)$ is the ordinary displacement operator. It is easy to get

$$\langle 0|D^+\hat{P}^2D|0\rangle=\frac{\hbar\sqrt{\mu}}{2}+p^2,$$
$$\langle 0|D^+\hat{X}^2D|0\rangle=\frac{\hbar}{2\sqrt{\mu}}+x^2, \tag{3.3}$$
$$\langle 0|D^+\hat{X}_i\hat{X}_{i-1}D|0\rangle=x_i x_{i-1},$$
$$\langle 0|D^+\cos(2\pi\hat{X})D|0\rangle=e^{-\hbar\pi^2/\sqrt{\mu}}\cos(2\pi x),$$

where $x=\langle 0|D^+\hat{X}D|0\rangle$ and $p=\langle 0|D^+\hat{P}D|0\rangle$ are the expectation values of the coordinate operator and the momentum operator of the ith atom, respectively. Thus we get the quantum Hamiltonian, the expectation value of the quantum Hamiltonian operator, as follows:

$$\overline{H}=\sum\left(\frac{3\hbar}{4\sqrt{\mu_i}}+\frac{p_i^2}{2\mu_i}+\frac{1}{2}(x_i-x_{i-1}-\gamma)^2 - \frac{K}{(2\pi)^2}e^{-\hbar\pi^2/\sqrt{\mu_i}}\cos(2\pi x_i)\right). \tag{3.4}$$

Variation with respect to p_i immediately yields $p_i/\mu_i=0$, and with respect to x_i yields

$$x_{i+1}-2x_i+x_{i-1}-\frac{K}{2\pi}e^{-\hbar\pi^2/\sqrt{\mu_i}}\sin(2\pi x_i)=0. \tag{3.5}$$

Let $y_{i+1}=x_{i+1}-x_i$, we get a two-dimensional area-preserving map,

$$x_{i+1}=x_i+y_{i+1},$$
$$y_{i+1}=y_i+\frac{K}{2\pi}e^{-\hbar\pi^2/\sqrt{\mu_i}}\sin(2\pi x_i). \tag{3.6}$$

Because of the correspondence between the ground states and the orbits of the area-preserving map, we can transcribe many results of the map to those of the generalized FK model.

A. Phase diagram in the (γ,K) space

Since the interatomic interaction is a convex function, we can use the gradient method,[7,10] Newton method,[10] to determine the periodic ground states.

For the generalized FK model, the values of the winding numbers in the classical phase diagram conform to the Farey tree structure, though their fraction forms do not. We expect that the values of the winding numbers in the quantum phase diagram also conform to the Farey tree structure. We construct the phase diagram of the system (3.1) in the following way: For a given commensurate state $\omega=P/Q$, where Q is always an *even number*, its left boundary is determined by equating the energies of the tongue and the incommensurate state $\overline{\omega}$ in its immediate left neighborhood. In practice, $\overline{\omega}$ is

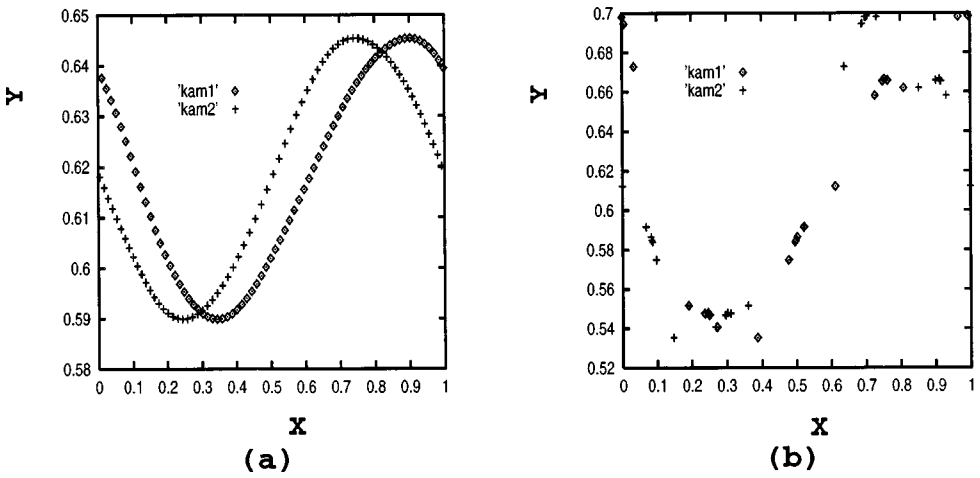

FIG. 3. Two examples of the KAM curves, where $\omega=\frac{89}{72}$ for map I_2I_1 or map I_1I_2, and $\omega=\frac{89}{144}$ for map (3.6); $\hbar=0.1$, $\mu=2$; $K=0.7$ in (a) and $K=2$ in (b). Here we use $\omega=\frac{89}{144}$ to approximate the golden mean winding number. To gain this figure, we use the Newton method to locate the ground state, then plot it in the (x,y) space. $KAM1$ is for the A subchain (also for map I_2I_1) and $KAM2$ is for the B subchain (also for map I_1I_2).

approximated by a left neighboring tongue $\omega=(Pm-1)/Qm$, where m is an equitable positive integer. The right boundary is determined in a similar way.

The average energy of each atom in the ground state is given by

$$h=\frac{1}{Q}\sum_{i=1}^{Q}\left(\frac{3\hbar}{4\sqrt{\mu_i}}-\frac{K}{(2\pi)^2}e^{-\hbar\pi^2/\sqrt{\mu_i}}\cos(2\pi x_i)+\frac{1}{2}(x_i-x_{i-1})^2\right)+\frac{\gamma^2}{2}-\frac{1}{Q}\sum_{i=1}^{Q}(x_i-x_{i-1})\gamma$$

$$\equiv h_l(\omega)+\frac{\gamma^2}{2}-\omega\gamma. \tag{3.7}$$

Let $h(\omega,\gamma_B)=h(\overline{\omega},\gamma_B)$, and we get

$$\gamma_B=\frac{h_l(\omega)-h_l(\overline{\omega})}{\omega-\overline{\omega}}. \tag{3.8}$$

When $\hbar\sim 0$, the boundaries of the tongues vary very slowly with μ. That is to say, the diatomic effects is very weak in this case. With the deepening of the quantization, the diatomic effects become strong. Figure 2 shows two examples, where only the tongues with $Q_A=Q_B\leqslant 5$ are shown. The tongues limited by the dashed lines are for the case of $\mu=1$ and the tongues limited by the solid lines are for the case of $\mu=5$. We use the winding number of the whole chain to describe the tongue. From left to right, the winding numbers are $\frac{0}{1}$, $\frac{2}{10}$, $\frac{1}{4}$, $\frac{2}{6}$, $\frac{4}{10}$, and $\frac{1}{2}$, respectively. $\hbar=0.01$ in (a) and $\hbar=0.1$ in (b). From Fig. 2 we expected that the threshold value K_c, at which the *transition by breaking of analyticity* occurs, increases with the deepening of the qauntization and decreases with the increasing of μ.

B. Map and critical point

It is easy to find that the map (3.6) reduces to the standard map if $\mu=1$. Otherwise, it can be decomposed as

$$I_1:\begin{cases} x_{2m} &= x_{2m-1}+y_{2m}, \\ y_{2m} &= y_{2m-1}+\dfrac{K}{2\pi}e^{-\hbar\pi^2}\sin(2\pi x_{2m-1}), \end{cases} \tag{3.9a}$$

$$I_2:\begin{cases} x_{2m+1} &= x_{2m}+y_{2m+1}, \\ y_{2m+1} &= y_{2m}+\dfrac{K}{2\pi}e^{-\hbar\pi^2/\sqrt{\mu}}\sin(2\pi x_{2m}). \end{cases} \tag{3.9b}$$

The equilibrium configurations of the A subchain correspond to the orbits of map I_2I_1, and the equilibrium configurations of the B subchain correspond to the orbits of map I_1I_2. When $\mu=1$, the Kolmogorov-Arnold-Moser (KAM) curve of I_1I_2 is identical to that of I_2I_1. When $\mu\neq 1$ the two KAM curves are different. The period of the orbit for map I_2I_1 or I_1I_2 is one half of that for the map (3.6), so the value of the winding number for map I_2I_1 or I_1I_2 is two times of that for the map (3.6) and it may be greater than 1. Figure 3 shows two examples of the KAM curves, where $\omega=\frac{89}{72}$ for map I_2I_1 or I_1I_2, and $\omega=\frac{89}{144}$ for map (3.6); $\hbar=0.1$, $\mu=2$; $K=0.7$ in (a) and $K=2$ in (b). Here we use $\omega=\frac{89}{144}$ to approximate the

TABLE I. Variation of K_c with $\hbar$ and μ.

	$\mu=1.0$	$\mu=1.2$	$\mu=1.4$	$\mu=1.6$	$\mu=1.8$	$\mu=2.0$
$\hbar=0.01$	1.072 422	1.005 991	0.984 596	0.956 965	0.947 970	0.924 304
$\hbar=0.1$	2.606 962	1.937 208	1.607 026	1.487 817	1.406 315	1.293 561

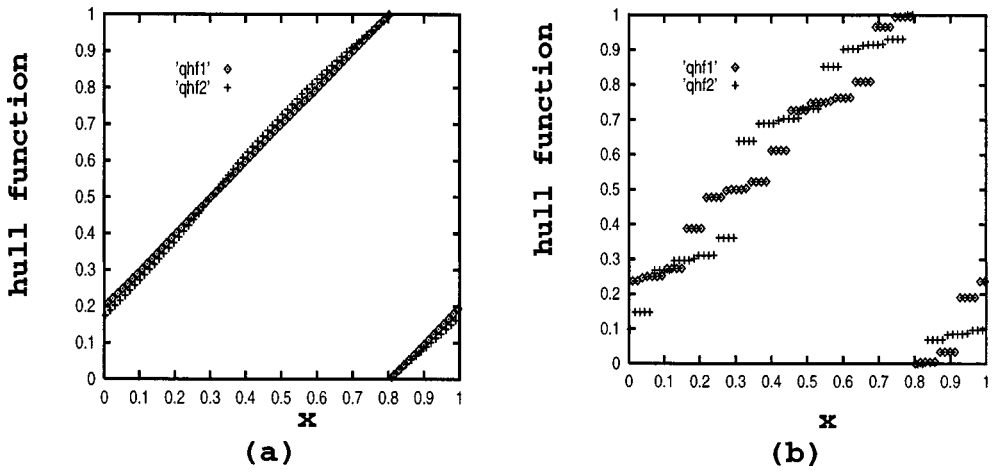

FIG. 4. Two examples of the quantum hull functions, where the values of parameters are just the same as those given in Fig. 3. ''$qhf1$'' is for the A subchain and ''$qhf2$'' is for the B subchain.

golden mean winding number. To gain this figure, we use the Newton method to locate the ground state, then plot it in the (x,y) space. $KAM1$ is for the A subchain (also for map I_2I_1) and $KAM2$ is for the B subchain (also for map I_1I_2).

It is easy to find that I_1 can be written as a product of two involutions $I_1=J_1J_2$, where

$$J_1\begin{pmatrix} x \\ y \end{pmatrix} = \begin{pmatrix} -x \\ y+\dfrac{K}{2\pi}e^{-\hbar\pi^2}\sin(2\pi x) \end{pmatrix},$$

$$J_2\begin{pmatrix} x \\ y \end{pmatrix} = \begin{pmatrix} y-x \\ y \end{pmatrix}. \tag{3.10}$$

Similarly, $I_2=J_3J_4$, where

$$J_3\begin{pmatrix} x \\ y \end{pmatrix} = \begin{pmatrix} -x \\ y+\dfrac{K}{2\pi}e^{-\hbar\pi^2/\sqrt{\mu}}\sin(2\pi x) \end{pmatrix},$$

$$J_4\begin{pmatrix} x \\ y \end{pmatrix} = \begin{pmatrix} y-x \\ y \end{pmatrix}. \tag{3.11}$$

Note that $J_1^2=J_2^2=J_3^2=J_4^2=1$ and $\det J_1=\det J_2=\det J_3=\det J_4=-1$. When $\mu=1$, $J_1=J_3$, $J_2=J_4$. Greene has observed that for any Q_i cycle at least two out of its Q_i points are fixed points of J_1 or J_2, and that the existence of the KAM curve is strongly connected with the stability of the Q_i cycles. He introduced two functions, $R_i^e(K)$ and $R_i^h(K)$, as the residues of the elliptic and hyperbolic Q_i cycles at a given value of K:

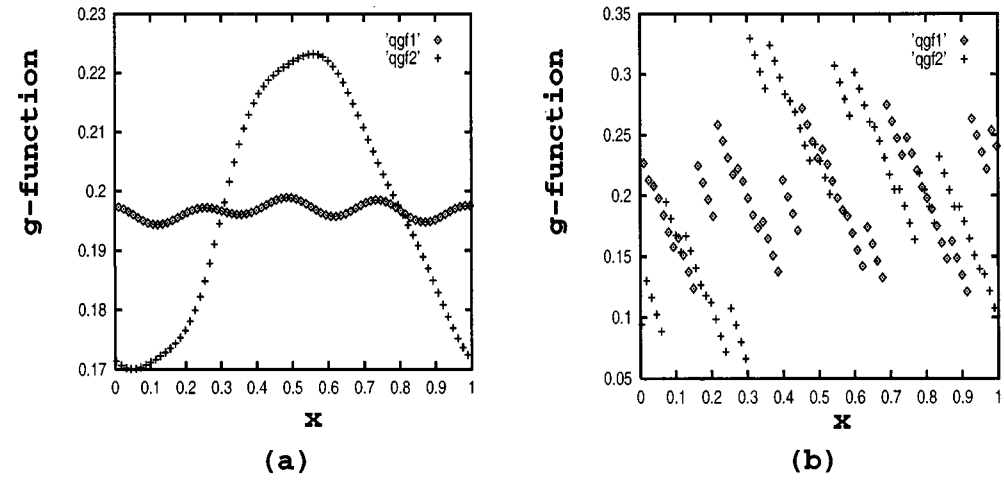

FIG. 5. Two examples of the quantum g functions, where the values of parameters are just the same as those given in Fig. 3. ''$qgf1$'' is for the A subchain and ''$qgf2$'' is for the B subchain.

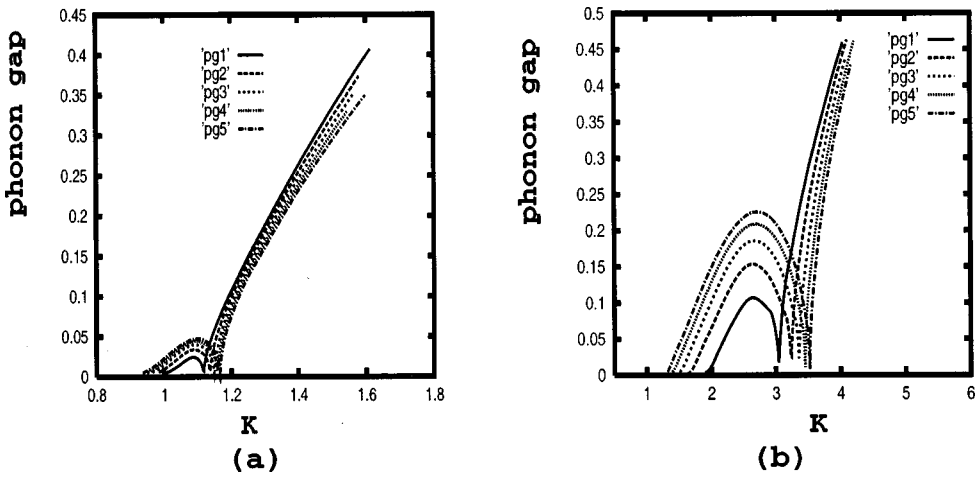

FIG. 6. Examples of the phonon gaps for $K>K_c$, where $\omega=\frac{89}{144}$ and $pg1$, $pg2$, $pg3$, $pg4$, $pg5$ correspond to the cases $\mu=1.2$, 1.4, 1.6, 1.8, and 2.0, respectively. $\hbar=0.01$ in (a) and $\hbar=0.1$ in (b). It is clear that the phonon gaps behave very differently from that of the standard FK model. There are two critical points, K_c and K_c', for each curve. When $K<K_c$, $\Omega_G=0$. When $K_c<K<K_c'$, Ω_G has a maximum value. When $K>K_c'$, Ω_G increases monotonically with K. K_c and K_c' both increases with the increasing of $\hbar$. With the increasing of μ, K_c decreases and K_c' increases. When $\hbar\to 0$ or $\mu\to 1$, $K_c'\to K_c$.

$$\lim_{i\to\infty} R_i^e(K)=\begin{cases}0^+, & K<K_c,\\ a, & K=K_c,\\ \infty, & K>K_c,\end{cases}$$

$$\lim_{i\to\infty} R_i^h(K)=\begin{cases}0^-, & K<K_c,\\ -b, & K=K_c,\\ -\infty, & K>K_c,\end{cases} \tag{3.12}$$

where a, b are positive constants less than unity. This provides an extremly accurate way to determine K_c. When $\mu\neq 1$, we expect that the map I_1I_2 and I_2I_1 have the same properties. The fixed points of J_1, J_2, J_3, and J_4 locate on the following four lines, respectively:

$$\begin{aligned}&\mathrm{a}=\{(x,y)|x=0\},\\ &\mathrm{b}=\left\{(x,y)|x=\frac{1}{2}\right\},\\ &\mathrm{c}=\left\{(x,y)|x=\frac{y}{2}\right\},\\ &\mathrm{d}=\left\{(x,y)|x=\frac{y+1}{2}\right\}.\end{aligned} \tag{3.13}$$

There are altogether four symmetry lines. The symmetries imply that the task of finding the Q_i cycle can be greatly simplified. We expect that the a line is the dominant symmetry line. After finding Q_i cycles one can calculate the values of R_i at the given values of K. Map I_1I_2 and map I_2I_1 have the same K_c for given $\hbar$ and μ. The value of K_c depends on the winding number. The KAM curve that breaks at last is the one with the golden mean winding number. For this curve, some examples of K_c are listed in Table I. It is clear that K_c increases with the increasing of $\hbar$ and with the decreasing of μ.

C. Hull function and transition by breaking of analyticity

In the absence of the external potential the equilibrium positions of atoms in the A subchain are given by

$$x_{2m-1}=(2m-1)\omega_A+\alpha, \tag{3.14}$$

the equilibrium positions atoms in the B subchain are given by

$$x_{2m}=(2m)\omega_B+\alpha, \tag{3.15}$$

where α is an arbitary phase. In the presence of the periodic external potential the equilibrium positions of atoms in the A subchain are given by a hull function,

$$\begin{aligned}x_{2m-1}=f_A[(2m-1)\omega_A+\alpha]&=(2m-1)\omega_A+\alpha\\ &+g_A[(2m-1)\omega_A+\alpha],\end{aligned} \tag{3.16}$$

and those in the B subchain are also given by a hull function,

TABLE II. Variation of K_c' with $\hbar$ and μ.

	$\mu=1.0$	$\mu=1.2$	$\mu=1.4$	$\mu=1.6$	$\mu=1.8$	$\mu=2.0$
$\hbar=0.01$	1.072 424	1.116 861	1.136 066	1.149 078	1.158 771	1.166 412
$\hbar=0.1$	2.606 962	3.048 760	3.236 015	3.361 974	3.454 558	3.526 437

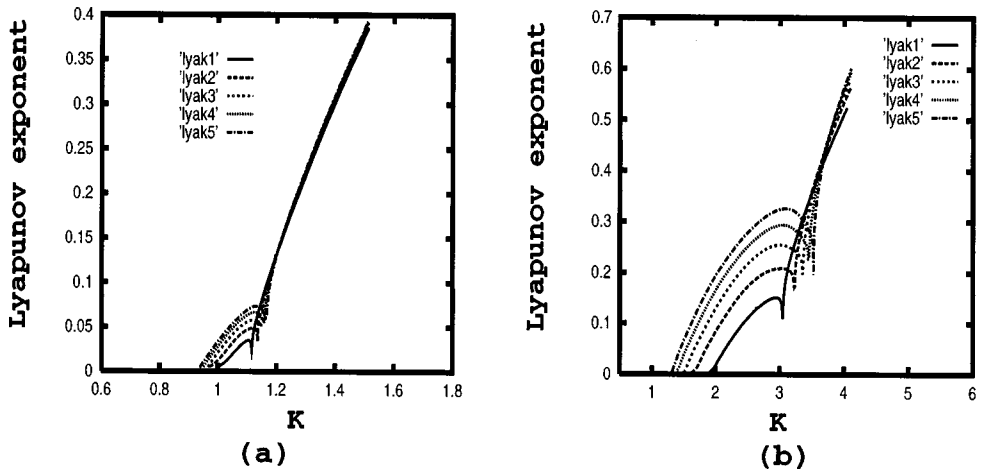

FIG. 7. Examples of the maximum Lyapunov exponents for $K>K_c$, where $\omega=\frac{288}{466}$ and $lyak1$, $lyak2$, $lyak3$, $lyak4$, $lyak5$ correspond to the cases $\mu=1.2$, 1.4, 1.6, 1.8, and 2.0, respectively. $\hbar=0.01$ in (a) and $\hbar=0.1$ in (b). The maximum Lyapunov exponents also behave very differently from that of the standard FK model. When $K<K_c$, $\gamma=0$. When $K_c<K<K_c'$, γ has a maximum value. When $K>K_c'$, γ increases monotonically with K.

$$x_{2m}=f_B[(2m)\omega_B+\alpha]=(2m)\omega_B+\alpha+g_B[(2m)\omega_B+\alpha], \tag{3.17}$$

where the g functions g_A and g_B are periodic with the same period as the external potential while the hull functions f_A and f_B are strictly increasing functions that depend on the winding number ω_A or ω_B. For the incommensurate phases, the properties of the hull functions and g functions are closely related to those of the KAM curves because they all describe the ground state. When $K<K_c$, the KAM curve with the winding number ω_A (or ω_B) does not break, so the corresponding hull function f_A (or f_B) is continuous. When $K>K_c$, the KAM curve with the winding number ω_A (or ω_B) breaks, so the corresponding hull function f_A (or f_B) is discontinuous. So does the corresponding g function. That is to say, *the transition by breaking of analyticity* occurs at K_c.

Figure 4 shows two examples of the quantum hull functions. Figure 5 shows two examples of two quantum g functions. Here the values of parameters are just the same as those given in Fig. 3. $qhf1$ and $qgf1$ are for the A subchain and $qhf2$ and $qgf2$ are for the B subchain.

D. Phonon gap, coherence length, and Peierls-Nabarro barrier

Similar to the classical model, many physical quantities also undergo a transition at K_c. In the following sections, we still study the three quantities, namely, phonon gap, coherence length, and the Peierls-Nabarro barrier.

1. Phonon gap

After considering the quantum effects, the eigenvalue equation of the square of the phonon frequency is

$$-\frac{\epsilon_{i-1}}{\mu_i}+\left(\frac{2+Ke^{-\hbar\pi^2/\sqrt{\mu_i}}\cos(2\pi x_i)}{\mu_i}-\Omega^2\right)\epsilon_i-\frac{\epsilon_{i+1}}{\mu_i}=0,$$

$$i=1,2,\cdots,Q. \tag{3.18}$$

For $K<K_c$, $x_i=f_i(i\omega+\alpha)$ is a static solution of equation $\partial H/\partial x_i=0$ for any phase α, where $f_i=f_A$ when $i=2m-1$ and $f_i=f_B$ when $i=2m$. Since $f_i(x)$ is an analytic function, inserting this solution in $\partial H/\partial x_i=0$ and differentiating this equation with respect to the phase α shows that

$$\epsilon_i=f_i'(i\omega+\alpha) \tag{3.19}$$

is a solution of Eq. (3.18) for $\Omega^2=0$. Consequently, for $K<K_c$ the gap in the phonon spectrum vanishes.

In contrast, for $K>K_c$, the hull function $f_i(x)$ becomes discrete with a derivative that is zero almost everywhere. Therefore Eq. (3.19) no longer defines an eigenmode for Eq. (3.18) with $\Omega^2=0$ and the gap in phonon spectrum Ω_G does not necessarily vanish. Figure 6 show some examples of the phonon gaps for $K>K_c$, where $\omega=\frac{89}{144}$ for the whole chain and $pg1$, $pg2$, $pg3$, $pg4$, $pg5$ correspond to the cases $\mu=1.2$, 1.4, 1.6, 1.8, and 2.0, respectively. $\hbar=0.01$ in (a) and $\hbar=0.1$ in (b). It is clear that the phonon gaps behave very differently from that of the standard FK model. There are two critical points, K_c and K_c', for each curve. When $K<K_c$, $\Omega_G=0$. When $K_c<K<K_c'$, Ω_G has a maximum value. When $K>K_c'$, Ω_G increases monotonically with K. K_c decreases and K_c' increases with the increasing of μ. K_c,

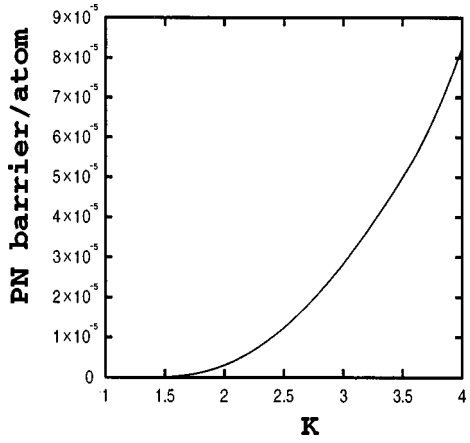

FIG. 8. Behavior of the PN barrier, where $\hbar=0.1$, $\mu=2$, $\omega=\frac{89}{144}$.

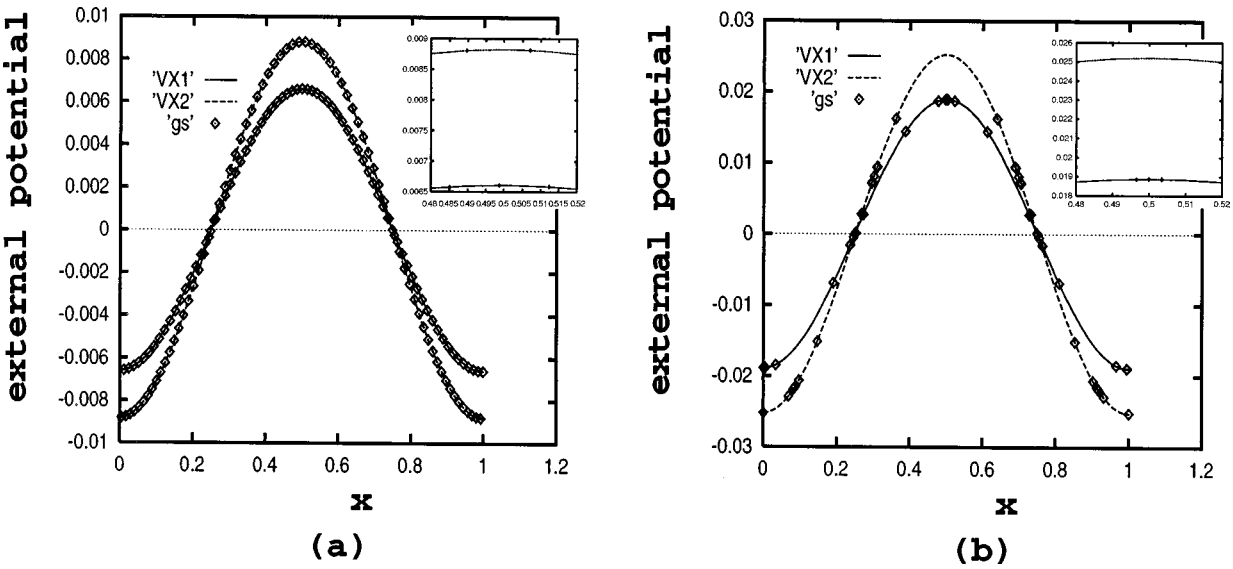

FIG. 9. Two examples of the ground states, where $\omega=\frac{89}{144}$, $\hbar=0.1$, $\mu=2$, and all the atoms denoted by ''$\diamond$'' are plotted in one period of the external potential. $K=0.7$ in (a) and $K=2$ in (b). ''$VX1$'' denotes the curve of $V(x)=-[K/(2\pi)^2]e^{-\hbar\pi^2}\cos(2\pi x)$ and ''$VX2$'' denotes the curve of $V(x)=-[K/(2\pi)^2]e^{-\hbar\pi^2/\sqrt{\mu}}\cos(2\pi x)$.

K_c' and the interval $[K_c,K_c']$ increases with the increasing of $\hbar$. When $\hbar\to 0$ or $\mu\to 1$, $K_c'\to K_c$. We use the greater systems to check and get the same result. We determine the value of K_c' in the light of the phonon gap. Some examples are shown in Table II.

Before we investigate the second critical point K_c', we first finish our study on the coherence length and the PN barrier.

2. Coherence length

The linear expansion of Eq. (3.5) yields:

$$\epsilon_{i+1}-[2+Ke^{-\hbar\pi^2/\sqrt{\mu_i}}\cos(2\pi x_i)]\epsilon_i+\epsilon_{i-1}=0,\quad (i\neq 0). \tag{3.20}$$

Equation (3.20) is identical to Eq. (3.18) where $\Omega=0$ and thus for $K<K_c$ it is satisfied by the solution (3.19). Consequently, we have

$$\epsilon_i=\frac{\epsilon_0}{f_0'(\alpha)}f_i'(i\omega+\alpha), \tag{3.21}$$

where $f_i'(x)$ is a positive continuous periodic function [$f(x)$ is analytic and strictly increasing]. As a consequence, ϵ_i has positive upper and lower bounds for $i\to\pm\infty$. From Eq. (2.13) we conclude that $\xi=\infty$ when $K<K_c$.

For $K>K_c$, define $\pi_{i+1}=\epsilon_{i+1}-\epsilon_i$, from Eq. (3.20) we have

$$\begin{pmatrix}\epsilon_{i+1}\\ \pi_{i+1}\end{pmatrix}=J_i\begin{pmatrix}\epsilon_i\\ \pi_i\end{pmatrix}, \tag{3.22}$$

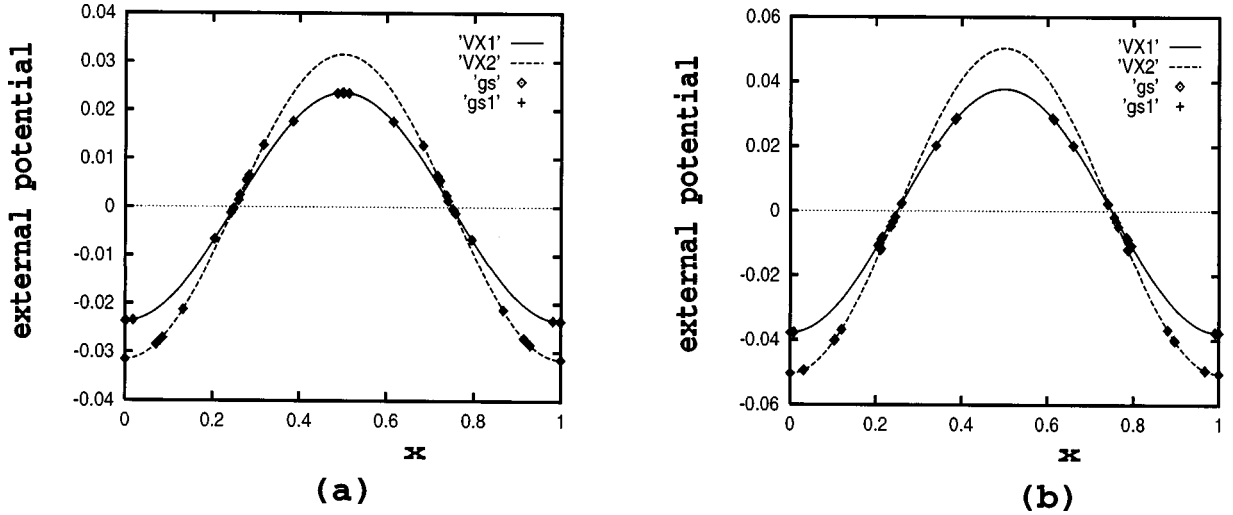

FIG. 10. Two other examples of the ground states, where $\hbar=0.1$, $\mu=2$, ''$gs1$'' denotes the ground state with $\omega=\frac{89}{144}$, and ''gs'' denotes the ground state with $\omega=\frac{1974}{3194}$. $K=2.5$ in (a) and $K=4$ in (b). From $\omega=\frac{89}{144}$ to $\omega=\frac{1974}{3194}$, the period of the ground state is enlarged by about twenty times, but there is no evident change that occurs in Ψ_A and Ψ_B.

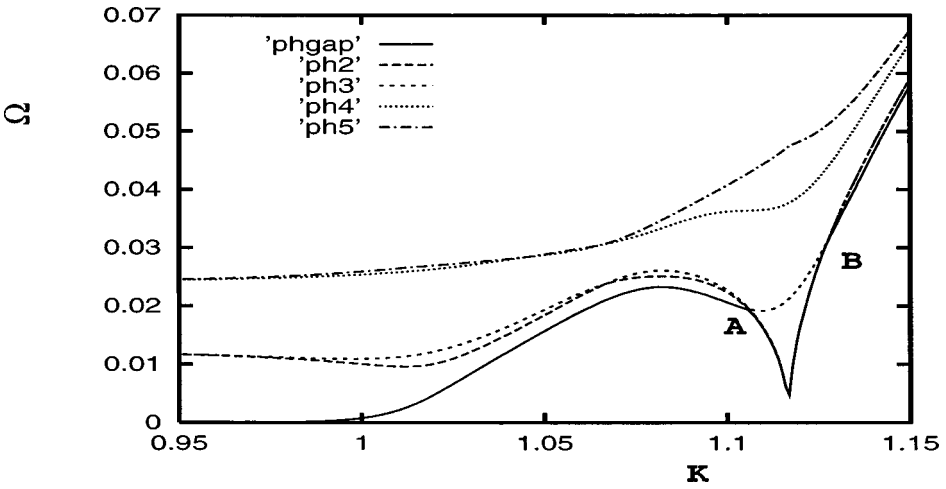

FIG. 11. Plot of Ω versus K, where $\hbar=0.01$, $\mu=1.2$, $\omega=\frac{288}{466}$. $phgap, ph2, ph3, ph4, ph5$ correspond to the phonon gap, the second minimum, the third minimum, the fourth minimum, and the fifth minimum of the phonon frequencies. There are two evident intersecting points, A and B, in the figure.

where

$$J_i=\begin{pmatrix} 1+Ke^{-\hbar\pi^2/\sqrt{\mu_i}}\cos(2\pi x_i) & 1 \\ Ke^{-\hbar\pi^2/\sqrt{\mu_i}}\cos(2\pi x_i) & 1 \end{pmatrix} \qquad (3.23)$$

is just the Jacobian matrix of the qauntum map (3.6). Thus we have $\xi=1/\gamma$, where γ is the maximum Lyapunov exponent in the quantum map. For $K>K_c$, γ is nonzero and behaves similar to the phonon gap. Figure 7 show some examples of the maximum Lyapunov exponents for $K>K_c$, where $\omega=\frac{288}{466}$ for the whole chain and $lyak1, lyak2, lyak3, lyak4, lyak5$ correspond to the cases $\mu=1.2$, 1.4, 1.6, 1.8, and 2.0, respectively. $\hbar=0.01$ in (a) and $\hbar=0.1$ in (b). The maximum Lyapunov exponents also behave very differently from that of the standard FK model. There are two critical points, K_c and K_c', for each curve. When $K<K_c$, $\gamma=0$. When $K_c<K<K_c'$, γ has a maximum value. When $K>K_c'$, γ increases monotonically with K. The numerical results show that the value of K_c' for the coherence length is just the same as that for the phonon gap. Owing to the numerical precision, we could not judge whether or not $\Omega_G=0$ or/and $\gamma=0$ when $K=K_c'$. If $\Omega_G=0$ and $\gamma=0$ at K_c', then a slide state occurs at K_c'.

3. Peierls-Nabarro barrier

For $K<K_c$, the PN barrier H_{PN} vanishes since no extra energy is needed to shift the chain in the sliding mode. For $K>K_c$, the ground state is described by a discontinuous hull function which in the (x,y) space is represented by a Cantor set. The PN barrier H_{PN} is the energy difference between the minimizing (min) orbit and its companion minimax (max) orbit. The numerical results show that the PN barrier only undergo a transition at K_c and behaves similarly to that of the standard FK model. Figure 8 shows an example of the behavior of PN barrier, where $\hbar=0.1$, $\mu=2$, $\omega=\frac{89}{144}$ for the whole chain. That is to say, there is no slide state that occurs at K_c', and $\Omega_G\neq 0$, $\gamma\neq 0$ at K_c'.

The PN barrier behaves very differently from the phonon gap and coherence length. The occurrence of K_c' does not affect the behavior of the PN barrier. To understand this feature, an investigation of K_c' is needed.

E. The second critical point K_c' and a new transition

It has been shown[10,22–24] that FK-type models with certain periodic potentials can have more than one transition (recurrence of KAM tori) for incommensurate states as the strength of the external potential is increased. In the following subsections, we will show that no KAM torus recurs and a new transition occurs at K_c' in the present model.

1. Configuration of the ground state

To understand the occurrence of K_c', we first investigate the configuration of the ground states. Figure 9 shows two examples of the ground states, where all the atoms denoted by ''$\diamond$'' are ploted in one period of the external potential, and all the values of the parameters are just the same as those given in Fig. 3. ''$VX1$'' denotes the curve of $V(x)=-[K/(2\pi)^2]e^{-\hbar\pi^2}\cos(2\pi x)$ and ''$VX2$'' denotes the curve of $V(x)=-[K/(2\pi)^2]e^{-\hbar\pi^2/\sqrt{\mu}}\cos(2\pi x)$. We define Ψ_A is the minimum distance from the A atoms to the top of $V(x)=-[K/(2\pi)^2]e^{-\hbar\pi^2}\cos(2\pi x)$, and define Ψ_B is the minimum distance from the B atoms to the top of $V(x)=-[K/(2\pi)^2]e^{-\hbar\pi^2/\sqrt{\mu}}\cos(2\pi x)$. Figure 10 shows two other examples of the ground states, where $\hbar=0.1$, $\mu=2$, ''$gs1$'' denotes the ground state with $\omega=\frac{89}{144}$, and ''gs'' denotes the ground state with $\omega=\frac{1974}{3194}$. $K=2.5$ in (a) and $K=4$ in (b). From $\omega=\frac{89}{144}$ to $\omega=\frac{1974}{3194}$, the period of the ground state is enlarged by about twenty times, but there is no evident change that occurs in Ψ_A and Ψ_B. For ground states with a certain winding number $\omega=P/Q$, where P and Q are finite Fibonacci numbers or both are two times of the corresponding Fibonacci numbers, the numerical results show that: (i) For B atoms, $\Psi_B>0$ and Ψ_B increases with K; (ii) For A atoms, K has two threshold values, K_c and K_c'. When $K<K_c$, $\Psi_A>0$ and Ψ_A decreases with the increasing of K. When $K_c<K<K_c'$, $\Psi_A=0$. When $K>K_c'$, $\Psi_A>0$ and Ψ_A increases with the increasing of K; (iii) When $K<K_c$, Ψ_A and Ψ_B both evidently decrease with the increasing of the size of the system; (iv) When $K_c\leqslant K\leqslant K_c'$, Ψ_A and Ψ_B do not vary with the size of the system; (v) When $K>K_c'$, Ψ_A and Ψ_B do not vary with the size of the system. Hence, the following conclusions for the incommensurate ground state with the golden mean winding number are reasonable: Ψ_A

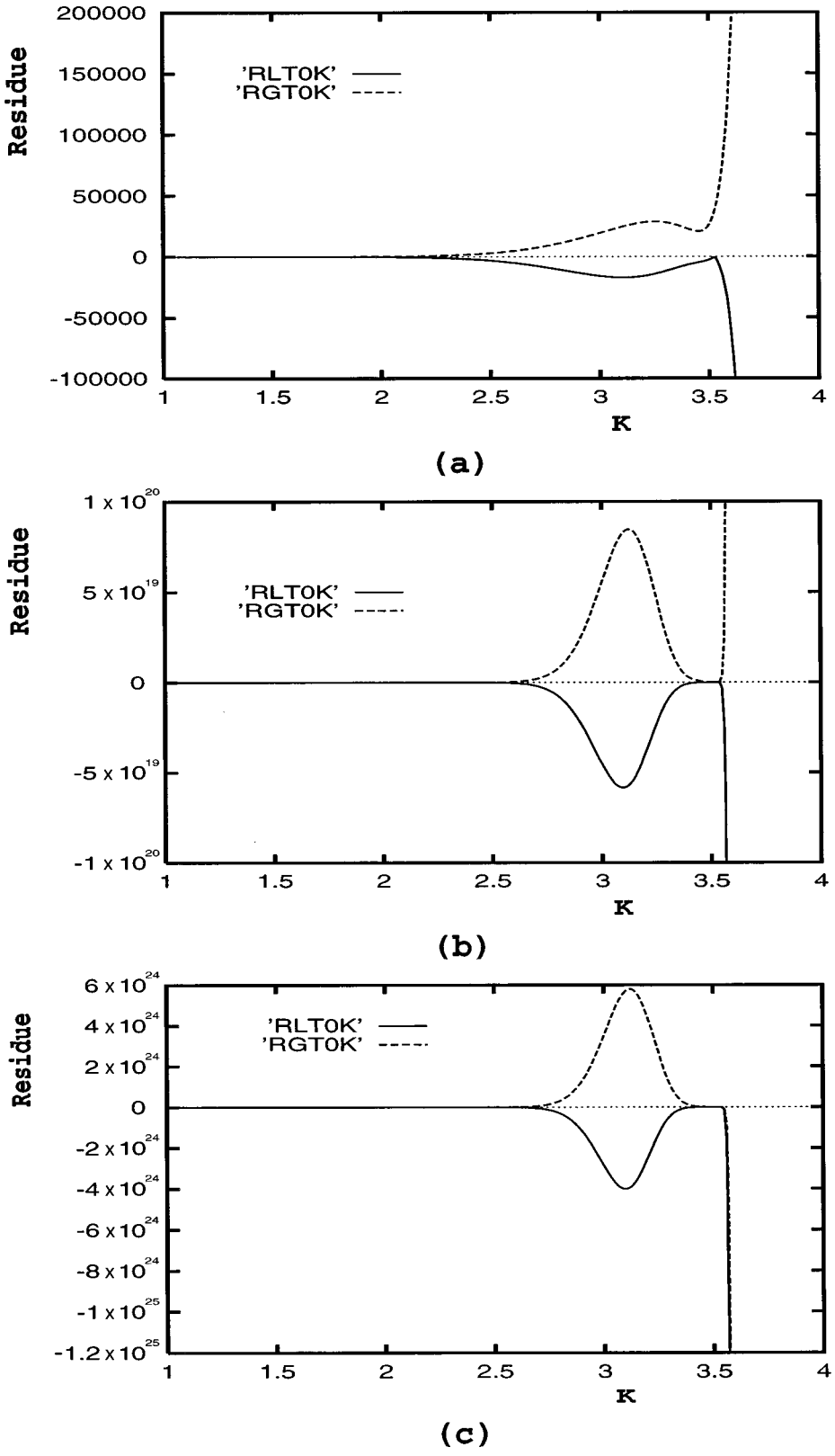

FIG. 12. Plot in the (residue, K) space, where the solid lines correspond to the minimizing orbit and the dashed lines correspond to the companion minimax orbit; $\hbar=0.1$, $\mu=2$; $\omega=\frac{21}{34}$ in (a), $\omega=\frac{89}{144}$ in (b), and $\omega=\frac{110}{178}$. The absolute values of the residues for the minimizing orbit first monotonically increases with K, then monotonically decreases with K, when $K>K_c'$ it again monotonically increases with K. The residue of the minimax orbit may change its sign at K_c', but for all the cases the residues of the minimizing orbit keep its sign.

$=0$ and $\Psi_B=0$ when $K<K_c$; $\Psi_A=0$ and $\Psi_B>0$ when $K_c<K<K_c'$; $\Psi_A>0$ and $\Psi_B>0$ when $K>K_c'$.

2. Minimal phonon frequencies

In order to understand the mechanism for the occurrence of the second critical point, we investigate the variation of the second minimum, third minimum, fourth minimum, and fifth minimum of the phonon frequencies, besides the phonon gap, with the increasing of the strength of the external potential. There are at least two different vibration modes that intersect in the (K,Ω) space, where Ω is the phonon frequency. Figure 11 shows an example, where $\hbar=0.01$, $\mu=1.2$, $\omega=\frac{288}{466}$. $phgap$, $ph2$, $ph3$, $ph4$, $ph5$ correspond to the phonon gap, the second minimum, the third minimum,

the fourth minimum, and the fifth minimum of the phonon frequencies, respectively. There are two evident intersecting points, A and B, in the figure. To gain the phonon gap, the second minimum, the third minimum, ..., of the phonon frequencies, we have to sort the phonon spectrum from small to big. When $\mu=1$, the present model reduces to the standard FK model, there is no intersection between different vibration modes in the (K,Ω) space. The diatomic effect results in the difference between the quantum modifications on different atoms, then results in a more complex interaction between different vibration modes.

3. Minimax orbit and minimizing orbit

To understand the occurrence of K_c' and to check whether or not the KAM torus may recur at K_c', we investigate the behaviors of the minimax orbit and the companion minimizing orbit around K_c'.

In the calculation of the PN barrier, the minimizing orbit (the ground state) is easy to find by using the Newton method. We need only to use the following initial configuration:[10]

$$x_i^0=\left(i\frac{P}{Q}\right), \quad i=1,2,\ldots,Q, \tag{3.24}$$

and a periodic condition

$$x_0=x_Q-P, x_{Q+1}=x_1+P \tag{3.25}$$

is imposed. That is to say, x_i^0 takes the integral part of iP/Q. The basic idea is to put the atoms initially in the valleys of the external potential. The system will then be trapped with certainty in the ground state before reaching a nonminimizing periodic orbit. To gain the companion minimax orbit, we start with a suitable K which is less K_c, using the following initial configuration:

$$x_i^0=\tfrac{1}{2}(x_i+x_{i+1}), \quad i=1,2,\ldots,Q, \tag{3.26}$$

where x_i is the gained minimizing orbit point. When we get the companion minimax orbit, then we use this configuration for the calculation of the next minimax orbit with a small increment in K.

Figure 12 shows three cases in the (residue, K) space, where the solid lines correspond to the minimizing orbit and the dashed lines correspond to the companion minimax orbit; $\hbar=0.1$, $\mu=2$; $\omega=\frac{21}{34}$ in (a), $\omega=\frac{89}{144}$ in (b) and $\omega=\frac{110}{178}$. The absolute values of the residues for the minimizing orbit first monotonically increases with K, then monotonically decreases with K, when $K>K_c'$ it again monotonically increases with K. The residue of the minimax orbit may change its sign at K_c', but for all the cases the residues of the minimizing orbit keep its sign. It does not satisfy the conditions for which the KAM torus can recur.

To identify the minimizing orbit corresponds to the ground state, we compared its energy with that of the companion minimax orbit for each value of K. We found that its energy is always the less one and the difference monotonically increases with K. So we believe that there is no KAM torus that recurs at K_c'.

IV. CONCLUSION

To understand the modulated structures and commensurate-incommensurate transitions, we generalize the Frenkel-Kontorova model to a diatomic chain in the presence of an external sinusoidal potential. For the classical ground states, the diatomic effect is reflected by the phase diagram and the phonon spectrum. The phase diagram of the classical ground state is just the same as that of the standard FK model in appearance. When the period of the ground state Q is an even number, the winding number is just the same as that of the standard FK model. When Q is an odd number, the winding number $\omega_g=2P/2Q$ if $\omega_s=P/Q$, where ω_g is for the generalized FK model and ω_s is for the standard FK model. The classical phonon spectrum is different from that of the standard FK model, but the critical exponent χ is just the same.

For the quantum ground states, the diatomic effects are reflected by the distribution of the atoms on the external potential, the phase diagram, correspondences between the ground states and the orbits of the area-preserving maps, the phonon spectrum, the coherence length, and the occurrence of a second critical point K_c' besides K_c at which the *transition by breaking of analyticity* occurs. When $K<K_c$, $\Psi_A=0$, $\Psi_B=0$, the phonon gap $\Omega_G=0$ and the Lyapunov exponent $\gamma=0$, the system is sliding. When $K_c<K<K_c'$, $\Psi_A=0$ and $\Psi_B>0$, so an extra energy is needed to shift the chain on the external potential, the system is pinned. Each of Ω_G and γ has a maximum value in this interval. When $K>K_c'$, $\Psi_A>0$ and $\Psi_B>0$, so more extra energy is needed to shift the chain, Ω_G and γ both increase monotonically with K. At the second critical point K_c', a new transition occurs. The behavior of the PN barrier is similar to that of the standard FK model. It is not affected by the occurrence of K_c'. With the deepening of the quantization, the diatomic effect becomes strong. With the increasing of $\hbar$, the differences between the phase diagrams for different μ become more prominent. The correspondences between the ground states and the orbits of the area-preserving maps are more complex than those of the standard FK model. The equilibrium configurations of the A subchain correspond to the orbits of map I_2I_1, and the equilibrium configurations of the B subchain correspond to the orbits of map I_1I_2. The critical points K_c and K_c' both increase with the increasing of $\hbar$. With the increasing of μ, K_c decreases and K_c' increases. The interval $[K_c,K_c']$ decreases with the decreasing of $\hbar$ or $\mu\to1$. When $\hbar=0$ or $\mu=1$, $K_c=K_c'$. We expect the results given in this paper to contribute to understanding the modulated structures and CI transitions in the complex lattice systems, especially in the systems with different particles.

ACKNOWLEDGMENTS

The work of Aiguo Xu, Guangrui Wang, and Shigang Chen was supported by the National Natural Science Foundation of China and the Science Foundation of China Academy of Engineering Physics. The work of Bambi Hu was supported in part by grants from the Hong Kong Baptist University (FRG) and the Hong Kong Research Grant Council (RGC).

[1] O. M. Braun and M. Peyrard, Phys. Rev. E **51**, 4999 (1995).
[2] T. Kontorova and Y. I. Frenkel, Zh. Eksp. Teor. Fiz. **8**, 89 (1938); **8**, 1340 (1938); **8**, 1349 (1938).
[3] J. B. Boyce and B. A. Huberman, Phys. Rep. **51**, 189 (1979).
[4] Y. I. Frenkel, *Introduction into the Theory of Metals* (Nauka, Leningrad, 1972).
[5] I. F. Lyuksyutov, A. G. Naumovets, and V. L. Pokrovsky, *Two-Dimensional Crystals* (Naukova Dumka, Kiev, 1988).
[6] A. S. Davydov, *Solitons in Molecular Systems* (Naukova Dumka, Kiev, 1984).
[7] S. Aubry, *Solitons and Condensed Matter Physics*, edited by A. R. Bishop and T. Schneider (Springer-Verlag, New York, 1978), p. 264; M. Peyrard and S. Aubry, J. Phys. C **16**, 1593 (1983); S. Aubry, Physica D **7**, 240 (1983); S. Aubry and P. Y. Le Daeron, *ibid.* **8**, 381 (1983); L. de. Seze and S. Aubry, J. Phys. C **17**, 389 (1984).
[8] S. N. Coppersmith and D. S. Fisher, Phys. Rev. B **28**, 2566 (1983).
[9] O. Biham and D. Mukamel, Phys. Rev. A **39**, 5326 (1989).
[10] B. Lin and B. Hu, J. Stat. Phys. **69**, 1047 (1992); J. Shi and B. Hu, Phys. Rev. A **45**, 5455 (1992); B. Hu, B. Lin, and J. Shi, Physica A **205**, 420 (1994); C. Chou, C. Ho, and B. Hu, Phys. Rev. E **55**, 5092 (1997).
[11] R. B. Griffiths and W. Chou, Phys. Rev. Lett. **56**, 1929 (1986); Phys. Rev. B **34**, 6219 (1986).
[12] A. Banerjea and P. L. Taylor, Phys. Rev. B **30**, 6489 (1984).
[13] M. Marchand, K. Hood, and A. Caile, Phys. Rev. Lett. **58**, 1660 (1987); Phys. Rev. B **37**, 1898 (1988).
[14] C. S. O. Yokoi, L.-H. Tang, and W. Chou, Phys. Rev. B **37**, 2173 (1988).
[15] Aiguo Xu, Guangrui Wang, Shigang Chen, and Bambi Hu, Phys. Rev. B **57**, 2771 (1998); Phys. Lett. A **233**, 99 (1997); Aiguo Xu, Guangrui Wang, and Shigang Chen, Chin. J. Comp. Phys. **14**, 521 (1997); Chin. Phys. Lett. **14**, 820 (1997); Chin. J. Comp. Phys. (to be published); Chin. J. Nonlin. Dyna. (to be published).
[16] O. M. Braun, Y. S. Kivshar, and A. M. Kosevich, J. Phys. C **21**, 3881 (1988); O. M. Braun, Y. S. Kivshar, and I. I. Zelenskaya, Phys. Rev. B **41**, 7118 (1990); O. M. Braun and Y. S. Kivshar, J. Phys.: Condens. Matter **2**, 5961 (1990); Phys. Rev. B **44**, 7694 (1991); O. M. Braun, O. A. Churbykalo, Y. S. Kivshar, and L. Vazquez, *ibid.* **48**, 3734 (1993); O. M. Braun, T. Dauxois, and M. Peyrard, *ibid.* **54**, 313 (1996); O. M. Braun, T. Dauxois, M. V. Paliy, and M. Peyrard, *ibid.* **54**, 321 (1996); See also Ref. 1.
[17] F. Borgonovi, I. Guarneri, and D. L. Shepelyansky, Phys. Rev. Lett. **63**, 2010 (1989); Z. Phys. B **79**, 133 (1990).
[18] G. P. Berman, E. N. Bulgakov, and D. K. Campbell, Phys. Rev. B **49**, 8212 (1994).
[19] Aiguo Xu, Guangrui Wang, Shigang Chen, and Bambi Hu, Commun. Theor. Phys. (to be published).
[20] S. Aubry, F. Axel, and F. Vallet, J. Phys. C **18**, 753 (1985).
[21] F. Axel and S. Aubry, J. Phys. A **20**, 4873 (1987).
[22] J. Wilbrink, Physica D **26**, 358 (1987).
[23] R. C. Black and I. I. Satija, Phys. Rev. A **40**, 2864 (1989).
[24] R. C. Black and I. I. Satija, Phys. Rev. Lett. **65**, 1 (1990).